# Instability prediction of brake squeal by nonlinear stability analysis

Zhi ZHANG[1]; Sebastian OBERST[2]; Joseph C.S LAI[3]

Acoustic and Vibration Unit, School of Engineering and Information Technology,

The University of New South Wales, ADFA, Canberra, ACT 2600, Australia

## ABSTRACT

Prediction of brake squeal as unwanted high frequency noise above 1 kHz remains a challenging problem despite substantial research efforts in the past two decades. Brake squeal, triggered by friction-induced self-excited vibration, can be caused by many different and interacting mechanisms with nonlinear origins in material properties and boundary conditions. Although brake squeal is essentially a nonlinear phenomenon, the standard industrial practice for prediction of brake squeal relies on the linear complex eigenvalue analysis which may under-predict or over-predict the number of unstable vibration modes. Brake squeal can be considered in nonlinear dynamics terms to be caused by a friction-induced self-excitation driven into instability and oscillating in a limit cycle through super-critical Andronov-Hopf bifurcations. In this paper, a nonlinear stability analysis that may be applied to a full brake system is examined using an unforced 4-DOF friction oscillator with cubic nonlinearity. The local bifurcation behaviour of this model is studied using the normal form theory and the nonlinear stability boundary is evaluated. Differences between results of linear and nonlinear analyses are discussed and the limitations of the linear analysis are highlighted. The energy provided by friction and consumed by damping is calculated by multiple scales method to provide a physical explanation for instability generation.

Keywords: Brake squeal, nonlinear stability analysis, friction work, damping work

## 1. INTRODUCTION

Brake squeal has been a major concern for automotive industry owing to the associated warranty costs and vehicle noise vibration and harshness performance (1). Several mechanisms are known to initiate brake squeal, e.g. negative gradient of the velocity- friction coefficient relationship, stick-slip, sprag-slip, hammering and mode coupling, etc (1, 2). A limit cycle may be established through friction-induced self-excited vibration, resulting in squeal (3). The most popular approach to determine unstable vibration modes is the complex eigenvalue analysis (CEA), which is a linear stability analysis. However, the CEA is often under-predictive owing to either modelling issues (correct friction law (4), sufficiently fine mesh in contact zone (2)) or over-predictive since not all unstable modes will squeal (5) or are able to radiate sound efficiently (3, 6). Further, linearization does not allow predicting all instabilities (4) or marginal unstable states (2) so that the results of CEA are neither necessary nor sufficient in predicting brake squeal.

One reason of the CEA's poor performance in many cases is that a brake system's noise performance might be nonlinearly correlated to its friction coefficient (5). Recently, the Ruelle -Takens route to chaos has been identified as a potential cause for brake squeal (6) which is a clear indication of nonlinearity in the system. Sources of nonlinearity are abundant in operating brake systems, e.g., the deflection of the lining material varies nonlinearly with the load (2), and detachment between the pad and the rotor (7), the nonlinear damping character of friction (8, 9), etc. Hence a nonlinear analysis of structural vibrations seems beneficial to understand the generation of instabilities.

The Normal Form Theory, as a nonlinear stability analysis approach, has been used to analyse a nonlinear brake model (3) to indicate that CEA is not sufficient for detecting instability. Using the Normal Form Theory, a nonlinear system can be reduced to a normal form (centre manifold reduction

[1] zhi.zhang3@student.adfa.edu.au
[2] s.oberst@adfa.edu.au
[3] j.lai@adfa.edu.au

(10), perturbation technique (11)) to qualitatively resemble the long term behaviour of the original system (11). In this work, a nonlinear stability analysis based on a perturbation approach (11) is applied to an analytical 4-DOF (degree of freedom) viscously-damped self-excited friction oscillator with cubic contact stiffness. The linear and nonlinear instability regions are predicted and compared. Friction work and viscous work over one cycle are calculated in order to highlight the feed-back energy as the physical origin of brake squeal (12, 13).

## 2. An analytical 4-DOF viscously-damped self-excited friction oscillator with cubic nonlinearity and stability analysis

A 4-DOF viscously-damped self-excited friction oscillator is shown in Figure 1. A block with mass $m_1$ and a conveyor belt with mass $m_2$ are held by linear springs with stiffness $k_{1\sim2}$ and $k_{3\sim4}$, respectively. A nonlinear spring with stiffness $k_5$ is used for modelling their contact. The spring force of $k_5$ is characterised as $F = k_{51}(y_1 - y_2) + k_{53}(y_1 - y_2)^3$, where $y_1 - y_2$ denotes the relative motion of $m_1$ and $m_2$ in the $y$ direction. $k_{51}$ and $k_{53}$ are two components of the stiffness $k_5$. The motion of the masses $m_1$ and $m_2$ in the $x$ and $y$ direction is viscously damped by dashpots of $c_2$, $c_3$ and $c_1$, $c_4$ respectively and coupled via constant friction coefficient $\mu$ using Coulomb-Amonton's law. In this model, the block $m_1$ and the conveyor $m_2$ represent the brake pad and brake rotor respectively while the spring $k_5$ represents the contact stiffness between the pad and the rotor. The $x$-direction is in the plane of the disc whereas the $y$-direction is out-of-plane.

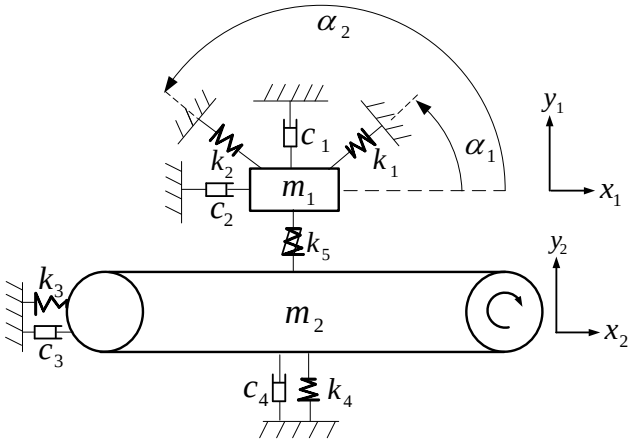


Figure 1- A viscously-damped self-excited nonlinear friction oscillator

Only the dynamics of the system in the steady sliding state is considered so that the stick-slip effect can be ruled out (14). The equations of motion be written as

$$\mathbf{M}\ddot{\mathbf{U}} + \mathbf{C}\dot{\mathbf{U}} + \mathbf{K}\mathbf{U} + \mathbf{F}_{Nl}(\mathbf{U}) = \mathbf{0} \tag{1}$$

with $\mathbf{U} = (x_1, y_1, x_2, y_2)^{\mathrm{T}}$ being the displacement vector and $\dot{(\,)}$ its time derivative. **M, C** and **K** are the diagonal mass, damping matrices and the asymmetric stiffness matrix respectively (15). $\mathbf{F}_{Nl}(\mathbf{U})$ is a vector containing the nonlinear expressions $(y_1 - y_2)^3 \cdot (-k_{53}\mu, k_{53}, k_{53}\mu, -k_{53})^{\mathrm{T}}$.

### 2.1 Linear stability analysis (CEA)

Perturbing the equilibrium point of Equation (1) and linearising the resultant nonlinear equations using a first-order Taylor expansion leads to a set of equations as

$$\mathbf{M}\ddot{\tilde{\mathbf{U}}} + \mathbf{C}\dot{\tilde{\mathbf{U}}} + \mathbf{K}\tilde{\mathbf{U}} = \mathbf{0} \tag{2}$$

The solution of Equation (2) is

$$\tilde{\mathbf{U}} = \sum_{j=1}^{4} e^{s_j t}\boldsymbol{\psi}_j \tag{3}$$

where $s_j$ and $\boldsymbol{\psi}_j$ are the $j^{\text{th}}$ complex eigenvalue and eigenvector of Equation. (2). If any $s_j$ has a positive real

part, the perturbed displacement $\tilde{\mathbf{U}}$ would exponentially increase indicating an instability. If there is at least one zero real part with all others being negative, the stability of the equilibrium point is not conclusive (16).

### 2.2 Nonlinear stability analysis

The system matrix of Equation (1) without nonlinear forces (17), can be transformed as (details in appendix A.1)

$$\ddot{z}_n + \omega_n{}^2 z_n = \varepsilon q_n(z_1,\ldots z_4,\dot{z}_1,\ldots \dot{z}_4) \tag{4}$$

$$q_n(z_1,\ldots z_4,\dot{z}_1,\ldots \dot{z}_4) = \sum_{l=1}^{4} 2\alpha_{nl}\dot{z}_l + \sum_{l=1}^{4}\beta_{nl}z_l{}^3 + \sum_{j=1}^{4}\sum_{l=1}^{4}\gamma_{nlj}z_l{}^2 z_j + \sum_{l=1}^{4}\sum_{j=1}^{4}\sum_{k=1}^{4}\delta_{nljk}z_l z_j z_k \text{ , } n=1\sim4, l\neq j\neq k \tag{5}$$

where $\varepsilon$ is a dimensionless small positive constant, representing the nonlinear stiffness characteristics of the brake lining; $z_n$ are the unknown variables; $\omega_n$ are the natural frequencies of the un-damped linear system; $\alpha_{ni}$ , $\beta_{ni}$ , $\gamma_{nij}$ and $\delta_{nijk}$ are known constants determined in the process of transformation (details in appendix A.2).

The solution of Equation (4) can be approximated by a truncated series in $\varepsilon$ (18)

$$z_n = \sum_{m=0}^{M}\varepsilon^m z_{nm}(\varepsilon^0 t,\ldots,\varepsilon^\infty t) \tag{6}$$

For small $\varepsilon$ , the nonlinearity is assumed to be weak, and those terms in Equation (6) of higher order will have diminishing contribution (12). Equation (6) can be truncated with two terms as

$$z_n = z_{n0}(T_0,T_1) + \varepsilon z_{n1}(T_0,T_1) + \mathrm{O}(\varepsilon^2) \tag{7}$$

where $T_0 = t$ , $T_1 = \varepsilon t$ are two time scales so that the derivative of a variable with time is written as (19)

$$\frac{d}{dt} = \frac{\partial}{\partial T_0} + \varepsilon\frac{\partial}{\partial T_1} = D_0 + \varepsilon D_1 \tag{8}$$

$$\frac{d^2}{dt^2} = D_0^2 + 2\varepsilon D_0 D_1 \tag{9}$$

Substituting Equation (7) into Equation (4) with the aid of Equations (8) and (9) and balancing the left and right hand side of the resultant equation according to the power of $\varepsilon$ leads to
The zeroth order of $\varepsilon$

$$D_0^2 z_{n0} + \omega_n{}^2 z_{n0} = 0 \tag{10}$$

The first order of $\varepsilon$

$$D_0^2 z_{n1} + \omega_n{}^2 z_{n1} = -2\sum_{l=1}^{4} D_0(D_1 z_{l0} + \alpha_{nl} z_{l0}) + \sum_{l=1}^{4}\beta_{nl}z_{l0}{}^3 + \sum_{j=1}^{4}\sum_{l=1}^{4}\gamma_{nlj}z_{l0}{}^2 z_{j0} + \sum_{l=1}^{4}\sum_{j=1}^{4}\sum_{k=1}^{4}\delta_{nljk}z_{l0}z_{j0}z_{k0} \tag{11}$$

The solution of Equation (10) is

$$z_{n0} = A_n(T_1)e^{i\omega_n T_0} + \overline{A_n}(T_1)e^{-i\omega_n T_0} \tag{12}$$

where $e$ is the exponential function and $i=\sqrt{-1}$. By substituting Equation (12) into Equation (11) the unknown variables $z_{n1}$ can now be solved in a closed form. By substituting $z_{n0}$ and $z_{n1}$ into Equation (7)). an approximate solution to the truncated original Equation (6) can be obtained..

However, to obtain a bounded solution of $z_{n1}$, the terms on the right hand side of Equation (11) with frequency equating to $\omega_n$ have to be artificially set as zero (so-called 'solvability condition' of perturbation techniques (7, 14), details in appendix A.3). The solvability condition would be a set of equations governing the amplitude $A_n(T_1)$ . If $A_n(T_1)$ reaches a non-zero steady state, the original nonlinear system is unstable.

## 3. Results and discussion

Results from the linear and the nonlinear stability analysis are compared by varying the friction coefficient $\mu$ and the spring stiffness $k_2$. The other values are set as $m_1$=1 kg, $m_2$=100 kg, $k_1$, $k_3$, $k_4$, $k_{51}$, $k_{53}$ are 2.49, 1, 1, 1.33, 1 N/m, $c_{1\sim4}$=0.05 Ns/m, $\alpha_1, \alpha_2$ are $30^0$ and $150^0$, respectively. These parameters values are chosen because, in a brake system, the mass of the rotor is typically about 100 times bigger than the mass of the pad. Other parameter values are chosen to be similar to those reported in Hoffmann et al. (20).

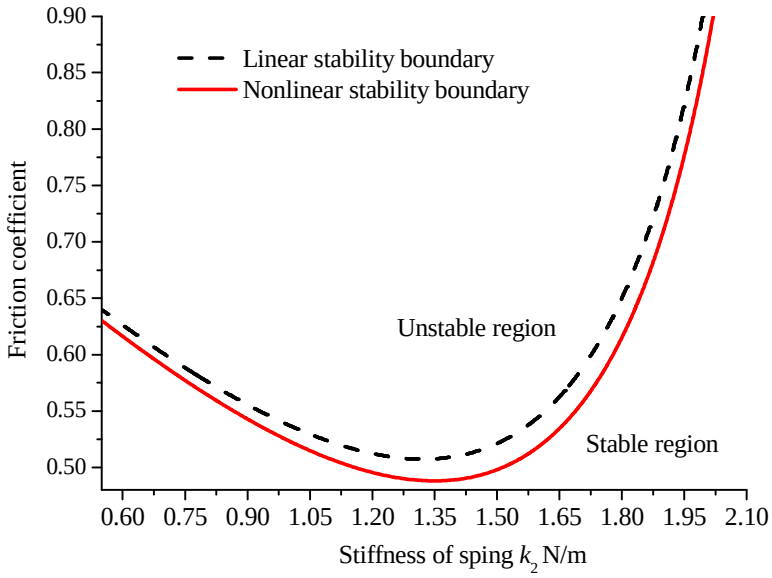


Figure 2 – Comparison between stable and unstable region predicted by linear (CEA) and nonlinear stability analysis

The stable and unstable region predicted by the CEA and nonlinear stability analysis is given in Figure 2. The nonlinear stability analysis predicts a larger area unstable region than the linear CEA highlighting the under-predictive character of the CEA as a squeal propensity assessment tool. Some area predicted to be stable by CEA is actually unstable in the nonlinear stability analysis. As predicted by the nonlinear stability analysis, every point in the region between the linear and nonlinear stability boundary in Figure 3 would show two possible solutions, one is stable as it decays to zero, while the other reaches a limit cycle (not predicted by CEA).

The 4$^{th}$ order Runge-Kutta method is applied to numerically integrate Eq.(1) with these points to check if a limit cycle can be reached By choosing an arbitrary point in the region between the linear and nonlinear stability boundary ( $\mu$ is 0.5 and the stiffness of spring $k_2$ are 1.21 N/m, respectively), the response of the 4-DOF friction oscillator indicates a periodically varying velocity (Figure 3).

By integrating the friction (& damping) forces along the path of the relative (absolute) displacement between $m_1$ and $m_2$ in the in-plane ($x$) direction, the friction (and damping) work over one cycle is calculated (Figure 4). The amount of work performed by friction and damping force (in absolute values) converges to about 2.45 J. This indicates that the energy provided by the friction force would balance the damped energy in the steady state, which is a necessary condition for the existence of a limit cycle (21). From the derivation of the solvability condition Equation (13), one could see closeness of natural frequencies would destabilise the dynamics in terms of the positive friction work while separation of circular frequencies would take the opposite effect (Appendix A.3).

## 4. Conclusions

Friction-induced self-excited vibration is usually considered as the primary cause of brake squeal. In this work, a linear and nonlinear stability analysis is performed to assess an analytical 4-DOF friction oscillator with cubic nonlinearity as a simplified brake model for predicting the instability region. Results show that either a nonlinear stability analysis or nonlinear time domain analysis is necessary to reliably predict the occurrence of a limit cycle. The linear stability analysis (CEA)

has been shown here to under-predict stability behaviour; not only chaotic regimes, but even limit cycles (6,7) might not be predicted numerically. In contrast to the linear the CEA (22), the nonlinear stability analysis is able to estimate the limit cycle's phase space diameter (3, 22, 23). The predicted instability is due to the positive work performed by friction force which is here the sole energy source leading to self-excitation (12). The nonlinear stability analysis has not been applied to a finite element model with many thousand DOFs due to its mathematical complexity and computational resources required; reduction methods are difficult to apply for nonlinear systems. Also, a priori knowledge of the type and the degree of nonlinearity is necessary and the effect of truncation of a series of solutions remains outstanding issues in brake squeal research.

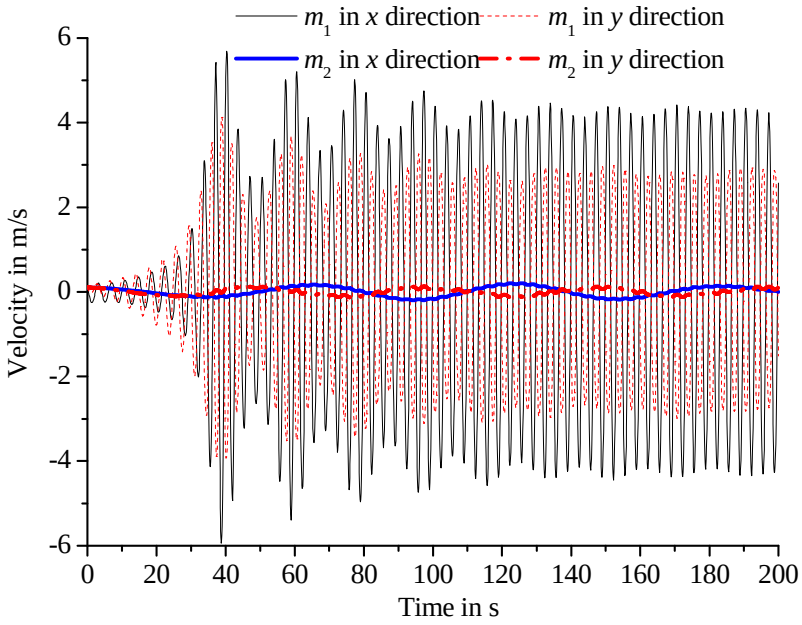


Figure 3. Velocity of the 4-DOF friction oscillator

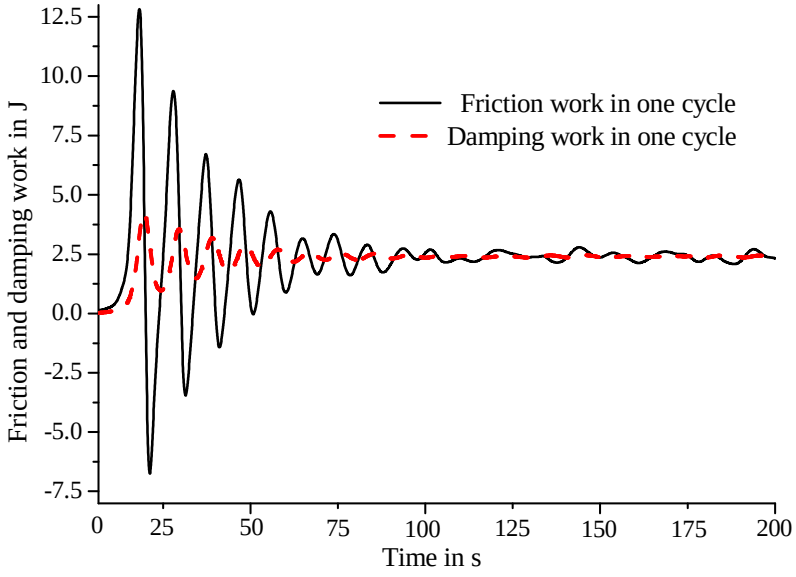


Figure 4. The evolution of friction and damping work per cycle

## ACKNOWLEDGEMENTS

The first author is grateful to be a recipient of the Australian Acoustical Society NSW Divison Travel Award and a University of New South Wales University College Postgraduate Research Scholarship for pursuing this study. This research was undertaken with the assistance of resources provided at the National Computational Infrastructure National Facility through the National Computational Merit Allocation Scheme supported by the Australian Government.

## REFERENCES


1. Kinkaid N, O'Reilly O, Papadopoulos P. Automotive disc brake squeal. Journal of sound and vibration. 2003;267(1):105-66.
2. Oberst SM. Analysis of brake squeal noise: University of New South Wales, Australian Defence Force Academy, School of Engineering and Information Technology.; 2011.
3. Hochlenert D. Nonlinear stability analysis of a disk brake model. Nonlinear Dynamics. 2009;58(1-2):63-73.
4. Tison T, Heussaff A, Massa F, Turpin I, Nunes R. Improvement in the predictivity of squeal simulations: Uncertainty and robustness. Journal of Sound and Vibration. 2014;333(15):3394-412.
5. Oberst S, Lai JCS. Statistical analysis of brake squeal noise. Journal of Sound and Vibration. 2011;330(12):2978-94.
6. Oberst S, Lai JCS. Chaos in brake squeal noise. Journal of Sound and Vibration. 2011;330(5):955-75.
7. Oberst S, Lai JCS, Marburg S. Guidelines for numerical vibration and acoustic analysis of disc brake squeal using simple models of brake systems. Journal of Sound and Vibration. 2013;332(9):2284-99.
8. Hetzler H. On the effect of nonsmooth Coulomb friction on Hopf bifurcations in a 1-DoF oscillator with self-excitation due to negative damping. Nonlinear Dynamics. 2012;69(1-2):601-14.
9. Hetzler H, Schwarzer D, Seemann W. Analytical investigation of steady-state stability and Hopf-bifurcations occurring in sliding friction oscillators with application to low-frequency disc brake noise. Communications in Nonlinear Science and Numerical Simulation. 2007;12(1):83-99.
10. Sinou JJ, Thouverez F, Jezequel L. Center manifold and multivariable approximants applied to non-linear stability analysis. International Journal of Non-Linear Mechanics. 2003;38(9):1421-42.
11. Yu P. Computation of normal forms via a perturbation technique. Journal of Sound and Vibration. 1998;211(1):19-38.
12. Von Wagner U, Schlagner S. On the origin of disk brake squeal. International Journal of Vehicle Design. 2009;51(1):223-37.
13. Guan D, Huang J. The method of feed-in energy on disc brake squeal. Journal of Sound and Vibration. 2003;261(2):297-307.
14. Zhang Z, Oberst S, Lai JC. Application of polynomial chaos expansions to analytical models of friction oscillators.
15. Papinniemi A. Vibro-acoustic studies of brake squeal noise: University of New South Wales, Australian Defence Force Academy, School of Aerospace, Civil and Mechanical Engineering; 2008.
16. Sinou JJ, Thouverez F, Jezequel L. Non-linear stability analysis of a complex rotor/stator contact system. Journal of Sound and Vibration. 2004;278(4-5):1095-129.
17. Chen S, Cheung Y, Lau S. On the internal resonance of multi-degree-of-freedom systems with cubic non-linearity. Journal of Sound and Vibration. 1989;128(1):13-24.
18. Lin C, Segel LA. Mathematics Applied to Deterministic Problems: SIAM; 1974.
19. Natsiavas S, Bouzakis K, Aichouh P. Free vibration in a class of self-excited oscillators with 1: 3 internal resonance. Nonlinear Dynamics. 1997;12(2):109-28.
20. Hoffmann N, Fischer M, Allgaier R, Gaul L. A minimal model for studying properties of the mode-coupling type instability in friction induced oscillations. Mechanics Research Communications. 2002;29(4):197-205.
21. Ding W. Self-Excited Vibration: Theory, Paradigms, and Research Methods: Springer; 2013.
22. Shin K, Brennan MJ, Oh JE, Harris CJ. Analysis of Disc Brake Noise Using a Two-Degree-of-Freedom Model. Journal of Sound and Vibration. 2002;254(5):837-48.
23. Massi F, Baillet L, Giannini O, Sestieri A. Brake squeal: Linear and nonlinear numerical approaches. Mechanical Systems and Signal Processing. 2007;21(6):2374-93.


## APPENDIX

### A.1 Transforming Equation (1) to Equation (4)

The left and right modal matrix $\mathbf{V}$ and $\mathbf{D}$ of the undamped linear part of Equation (1) can be determined as an eigenvalue problem by

$$\mathbf{K}^{\mathbf{T}}\mathbf{V} = \lambda_V \mathbf{M}^{\mathbf{T}}\mathbf{V}\ ,\ \mathbf{KD} = \lambda_D \mathbf{MD} \tag{A.1}$$

where $\lambda_V$ and $\lambda_D$ are the corresponding eigenvalues.

Transforming the original unknown vector by using $\mathbf{U} = \mathbf{DZ}$ and substituting it into Equation (1), then left- multiplying $\mathbf{V}^{\mathrm{T}}$, one obtains

$$\mathbf{V}^{\mathrm{T}}\mathbf{MD}\ddot{\mathbf{Z}} + \mathbf{V}^{\mathrm{T}}\mathbf{KDZ} = -\mathbf{V}^{\mathrm{T}}\mathbf{CD}\dot{\mathbf{Z}} + \mathbf{V}^{\mathrm{T}}(\mathbf{K_f DZ})^3 \tag{A.2}$$

where

$$\mathbf{K_f} = \begin{bmatrix} 0 & k_{53}\mu & 0 & -k_{53}\mu \\ 0 & -k_{53} & 0 & k_{53} \\ 0 & -k_{53}\mu & 0 & k_{53}\mu \\ 0 & k_{53} & 0 & -k_{53} \end{bmatrix} \tag{A.3}$$

$\mathbf{K}_{\mathrm{f}}$ represents the friction and normal force acting on $m_1$ and $m_2$ due to the nonlinear element of the model. Left-multiplying Equation (A.2) by the invers matrix of $\mathbf{V}^{\mathrm{T}}\mathbf{MD}$ leads to

$$\ddot{\mathbf{Z}} + (\mathbf{V}^{\mathrm{T}}\mathbf{MD})^{-1}(\mathbf{V}^{\mathrm{T}}\mathbf{KD})\mathbf{Z} = -(\mathbf{V}^{\mathrm{T}}\mathbf{MD})^{-1}(\mathbf{V}^{\mathrm{T}}\mathbf{CD})\dot{\mathbf{Z}} + (\mathbf{V}^{\mathrm{T}}\mathbf{MD})^{-1}\mathbf{V}^{\mathrm{T}}(\mathbf{K_f DZ})^3 \tag{A.4}$$

Equation (4) is just an abbreviation of Equation (A.4).

### A.2 Determination of the coefficients in Eq. (5)

Equation (5) is the right hand side of Equation (A.4) and it takes the form as

$$q_n(z_1,\ldots z_4,\dot{z}_1,\ldots \dot{z}_4) = \sum_{l=1}^{4} 2\alpha_{nl}\dot{z}_l + \sum_{l=1}^{4}\beta_{nl}{z_l}^3 + \sum_{j=1}^{4}\sum_{l=1}^{4}\gamma_{nlj}{z_l}^2 z_j + \sum_{l=1}^{4}\sum_{j=1}^{4}\sum_{k=1}^{4}\delta_{nljk} z_l z_j z_k \quad \text{, n=1~4} \tag{A.5}$$

The value of $\alpha_{nl}$ is determined by just multiplying the element locates at the $n^{\text{th}}$ row and $l^{\text{th}}$ column of matrix $-(\mathbf{V}^{\mathrm{T}}\mathbf{MD})^{-1}(\mathbf{V}^{\mathrm{T}}\mathbf{CD})$ with -0.5. Determination of $\beta_{nl}$, $\gamma_{nlj}$, $\delta_{nljk}$ requires first expanding the $(\mathbf{V}^{\mathrm{T}}\mathbf{MD})^{-1}\mathbf{V}^{\mathrm{T}}(\mathbf{K_f DZ})^3$ and then determining the corresponding coefficients.

### A.3 Determination of solvability condition

Take Eq. (11) as an example:

$$D_0^2 z_{11} + {\omega_1}^2 z_{11} = -2\sum_{l=1}^{4} D_0(D_1 z_{l0} + \alpha_{1l} z_{l0}) + \sum_{l=1}^{4}\beta_{1l}{z_{l0}}^3 + \sum_{j=1}^{4}\sum_{l=1}^{4}\gamma_{1lj}{z_{l0}}^2 z_{j0} + \sum_{l=1}^{4}\sum_{j=1}^{4}\sum_{k=1}^{4}\delta_{1ljk} z_{l0} z_{j0} z_{k0} \tag{A.5}$$

By imposing the solvability condition eliminates all the terms on the right hand side of Equation (A.5) which include the circular frequency $\omega_1$.

As $z_{10}$ has been obtained in Eq. (12) as

$$z_{10} = A_1(T_1)e^{i\omega_1 T_0} + \overline{A_1}(T_1)e^{-i\omega_1 T_0} \tag{A.6}$$

Then the first term on the right hand side of Eq. (A.5) would become

$$\begin{aligned} -2\sum_{l=1}^{4} D_0(D_1 z_{l0} + \alpha_{1l} z_{l0}) = {} & -2i\omega_1(D_2 A_1 + \alpha_{11}A_1)e^{i\omega_1 T_1} - 2i\omega_2(D_2 A_2 + \alpha_{12}A_2)e^{i\omega_2 T_1} \\ & - 2i\omega_3(D_2 A_3 + \alpha_{13}A_3)e^{i\omega_3 T_1} - 2i\omega_4(D_2 A_4 + \alpha_{14}A_4)e^{i\omega_4 T_1} \end{aligned} \tag{A.7}$$

The second term on the right hand side of Eq. (A.5) would become

$$\begin{aligned} \sum_{l=1}^{4}\beta_{1l}{z_{l0}}^3 = {} & \beta_{11}({A_1}^3 e^{i3\omega_1 t} + 3{A_1}^2\overline{A_1}e^{i\omega_1 t} + 3A_1\overline{A_1}^2 e^{-i\omega_1 t} + \overline{A_1}^3 e^{-i3\omega_1 t}) \\ & + \beta_{12}({A_2}^3 e^{i3\omega_2 t} + 3{A_2}^2\overline{A_2}e^{i\omega_2 t} + 3A_2\overline{A_2}^2 e^{-i\omega_2 t} + \overline{A_2}^3 e^{-i3\omega_2 t}) \\ & + \beta_{13}({A_3}^3 e^{i3\omega_3 t} + 3{A_3}^2\overline{A_3}e^{i\omega_3 t} + 3A_3\overline{A_3}^2 e^{-i\omega_3 t} + \overline{A_3}^3 e^{-i3\omega_3 t}) \\ & + \beta_{14}({A_4}^3 e^{i3\omega_4 t} + 3{A_4}^2\overline{A_4}e^{i\omega_4 t} + 3A_4\overline{A_4}^2 e^{-i\omega_4 t} + \overline{A_4}^3 e^{-i3\omega_4 t}) \end{aligned} \tag{A.8}$$

As can be seen in Eq. (A.7- A.8), $-2i\omega_1(D_2 A_1 + \alpha_{11}A_1) + 3\beta_{11}{A_1}^2\overline{A_1}$ has to be set as zero. Similarly, we can find other terms with the circular frequency of $\omega_1$ from the left two terms on the right hand side of Eq. (A.5) and in conjunction with $-2i\omega_1(D_2 A_1 + \alpha_{11}A_1) + 3\beta_{11}{A_1}^2\overline{A_1}$, this constitutes the solvability condition for Eq. (A.5).

If $\omega_1 \approx \omega_2$ (mode coupling), additional terms like $3\beta_{12}{A_2}^2\overline{A_2}$ will come into the solvability condition which in turn influences the amplitude of the solution ($A_1$). For a certain parameter combination, a stable nontrivial $A_1$ bifurcates which is related to a super-critical Hopf bifurcation.